

The crystal structure of γ -P₄, a low temperature modification of white phosphorus

Hiroki Okudera*, Robert E. Dinnebier and Arndt Simon

Max-Planck-Institut für Festkörperforschung, Heisenbergstraße 1, D-70569 Stuttgart, Germany

Dedicated to Professor Dr. Hans-Jörg Deiseroth on the occasion of his 60th birthday

Received June 8, 2004; accepted August 3, 2004

*White phosphorus / P₄ γ -modification /
Distorted bcc packing / Lone pairs /
Powder diffraction structure analysis / X-ray diffraction*

Abstract. The crystal structure of γ -P₄, one of three modifications hitherto reported on white phosphorus, was determined from X-ray powder diffraction data collected at $T = 123$ K on a Guinier-Simon camera equipped with a cold gas blower and an image plate detector. Crystallographic data at $T = 123$ K are: space group $C2/m$, $a = 9.1709(5)$ Å, $b = 8.3385(5)$ Å, $c = 5.4336(2)$ Å, and $\beta = 90.311(3)^\circ$, $V = 415.51(6)$ Å³, $Z = 4$. The crystal structure of γ -P₄ was solved by the method of simulated annealing. The subsequent Rietveld refinement in the range $12^\circ < 2\theta < 92^\circ$ employing rigid-body constraints on the P₄ molecule converged at $R_p = 3.8$, $wR_p = 5.0$, and $R_F^2 = 14.0\%$. The asymmetric unit of γ -P₄ contains three P atoms; two P atoms in a molecule are related by a mirror plane which bisects the molecule. The centers of gravity of these P₄ molecules show a distorted body-centered cubic arrangement. The four apices of the P₄ tetrahedron point to the largest possible voids formed by neighbor molecules. The difference to the crystal structures of SiF₄ and GeF₄ with an exact bcc arrangement of tetrahedral molecules is discussed as well as, in terms of layer stackings, the similarity of the structures of γ - and β -P₄.

1. Introduction

White phosphorus, composed of P₄ molecules is the most reactive allotrope of the element, and it exists as three modifications at different temperatures and pressures. The room temperature modification called α -P₄ is a plastic crystal with the P₄ molecules dynamically rotating around their centers of gravity. The arrangement of these molecules was confirmed to be identical with the atomic arrangement in the α -Mn structure [1]. One of two low temperature modifications is called β -P₄. This modification is

stable below 197 K at ambient pressures or higher than 1.0 GPa at ambient temperature [2]. In the crystal structure of β -P₄ (space group $P\bar{1}$ [3]), the molecules have fixed orientations. The existence of yet another low temperature modification called γ -P₄ was first reported by Spiess et al. [4]. It was discovered by NMR measurements on white phosphorus at around 108 K. Phase relationships among these three modifications at ambient pressure were established by DTA and X-ray powder diffraction experiments [3]. α -P₄ can be supercooled by rapid quenching from room to liquid nitrogen temperature. The α -modification soon transforms to γ -P₄ upon slow warming. This γ -modification then exists as a stable lower temperature modification up to approximately 160 K. At higher temperatures it irreversibly transforms to β -P₄, and finally β -P₄ reversibly transforms back to α -P₄ at a temperature of about 193 K. However, when quenching is not fast enough, the α -P₄ sample directly transforms to β -P₄. In this paper, we report on the structure solution for γ -P₄ from X-ray powder diffraction experiments. The atomic arrangement and the crystal packing of γ -P₄ as well as the structural relationship between β - and γ -P₄ are discussed.

2. Experimental details and results

2.1 Sample preparation

Since white phosphorus is sensitive to visible light and oxidizes spontaneously in air, the sample preparation was performed under red light in argon atmosphere. A sample of α -P₄ was cut out under water from the central part of a rod of commercial white (yellow coloured) phosphorus, introduced into a specially designed glass apparatus with fused-on glass capillaries of 0.1–0.3 mm in diameter and dried in an argon stream. The raw material was distilled three times in a vacuum of $p = 10^{-2}$ torr and finally collected as a highly refractive colorless solid. A part of this purified α -P₄ was melted and manipulated into the capillaries under argon taking care that the length of the X-ray sample stayed short, approximately 5 mm, in order to cool fast enough to avoid the formation of β -P₄.

* Correspondence author (e-mail: H. Okudera@fkf.mpg.de)

2.2 Data collection

X-ray diffraction intensities were collected on an image plate (IP) installed in a Guinier-Simon camera [5] equipped with a N_2 -gas stream cooling device [6] which allows very fast quenching. The incident X-ray beam was monochromatized by a quartz Johannson-type monochromator, and $CuK\alpha_1$ radiation was employed for data collection. The temperature was set with a precision of $\Delta T = 0.02$ K at the sample position, and fluctuation was kept less than $\Delta T = \pm 0.05$ K by a PID controller [5]. The correction coefficient for the effective camera radius was preliminarily determined using silicon powder as an external standard (99.9995% Si powder, Aldrich; $a = 5.4309$ Å at $T = 293$ K [7]). No internal standard was used at data collection. Further details of experimental set-ups of the camera and diffraction geometry are described in Refs. [3, 5].

The capillary sample (0.3 mm diameter) was mounted on the camera and rotated during exposures. Firstly, the sample was quenched from room temperature to 93 K by quickly removing a piece of paper, which kept the cold N_2 -gas stream away from the sample. Initial IP exposure was made at this stage to check, whether the sample was still in the α -modification. Secondly, after confirming that the sample retained its α -modification, a ΔT diagram was collected by slowly shifting the IP (exposure 1) while the temperature was slowly increased from $T = 93$ to 290 K at a rate of 11.4 K/h. A second quenching cycle was started using the same sample, and a powder diffraction pattern of γ - P_4 was collected with a fixed IP detector at $T = 123$ K for 17 hours (exposure 2). The IP was read out by a Fuji BAS-5000 IP reader system with provided software, resulting in diffraction intensities versus angle.

2.3 Phase transitions on the ΔT diagram

The ΔT diagram (exposure 1) is shown in Fig. 1a. On this diagram it can clearly be seen that at $T = 93$ K the sample was already transformed to γ - P_4 , and the γ to β phase transition occurred at $T = 155$ K, and that the β to α transition occurred at $T = 187$ K. High angle diffraction lines from γ - and β - P_4 are now clearly visible on the diagram, while those from α - P_4 are still insignificant. The large overlaps of diffraction lines from different modifications

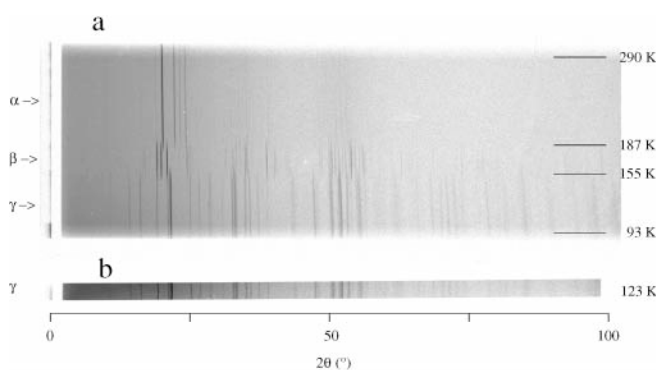


Fig. 1. X-ray powder diffraction profiles collected on a Guinier-Simon camera equipped with IP detector. (a) ΔT diagram of a quenched sample with increasing temperature (exposure started from the bottom; exposure 1). (b) Fixed-IP and fixed-temperature exposure on γ - P_4 sample at $T = 123$ K (exposure 2).

on the IP image around the transition temperatures were due to the slit width of 6 mm in front of the film, while the sample transformed sharply at these transition points. The slit width also caused some broadening of the diffraction lines on the ΔT diagram in comparison to the static IP exposure at constant temperature (Fig. 1b).

2.4 Profile decomposition and cell determination

Individual peak fitting using the split-type pseudo-Voigt line shape function [8] in the program PRO-FIT [9] was used to find 33 possible peak positions up to $2\theta = 76^\circ$ from the diffraction pattern collected at $T = 123$ K (exposure 2). The peak positions were subjected to a unit cell search by the CRYSFIRE peak indexing program package [10]. A C -centered monoclinic unit cell was found with cell dimensions of $a = 9.16$ Å, $b = 8.33$ Å, $c = 5.43$ Å, and $\beta = 90.35^\circ$. This monoclinic cell was confirmed by whole-powder-pattern fitting program WPPF [9]. Observed systematic extinctions indicated either $C2$, Cm or $C2/m$ as possible crystallographic space groups.

2.5 Structure solution

The crystal structure of γ - P_4 was solved using the DASH crystal structure solution package [11] utilizing the simulated annealing technique [12]. In this calculation, the measured powder pattern (exposure 2) was subjected to a Pawley refinement [13] in space groups $C2$, Cm and $C2/m$ in order to extract correlated integrated intensities from the pattern. The structure was solved under assumption of four P_4 molecules per unit cell from the volume of a single P_4 molecule in the α - and β - P_4 structures [1, 3]. An internal coordinate description of the P_4 tetrahedron was taken from β - P_4 [3]. The position and orientation of only one kind of P_4 tetrahedron in the cell were postulated. The trial structure was subjected to a global optimization [10] without internal degrees of freedom. The external degrees of freedom consisted of the fractional coordinates describing the center of gravity position of the P_4 tetrahedron, and four quaternions [14] describing the orientation of the molecule. The structure giving the best fit to the data was

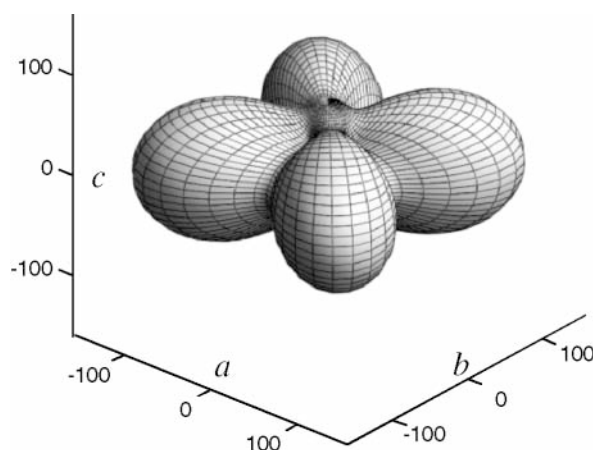


Fig. 2. Three-dimensional strain distribution of γ - P_4 at $T = 123$ K. The distance from the origin to the surface represents the size of microstrain, and directions with large strain values represent "soft" directions. The scale is in $\delta d/d \times 10^{-6}$.

Table 1. Crystallographic data, conditions and results of Rietveld structure refinement.

Crystallographic data	
Formula	P ₄
Temperature	123 K
Mole mass	123.895 a.m.u.
Space group; No.	<i>C2/m</i> (no. 12)
Z	4
<i>a</i>	9.1709(5) Å
<i>b</i>	8.3385(5) Å
<i>c</i>	5.4336(2) Å
β	89.689(3) °
<i>V</i>	415.51(6) Å ³
ρ -calc	1.981 g cm ⁻³
Rietveld refinement	
Wavelength	1.54059 Å (CuK α_1)
Capillary diameter	0.3 mm
Absorption coefficient	149.6 cm ⁻¹
2 θ range analyzed	12–92 °
Exposure time	17 h
No. of observations	3200
No. of reflections	199
Parameters refined	37
R_p	0.050
wR_p	0.038
R_F^2	0.140

Table 2. Atomic parameters and displacement parameters of γ -P₄ at $T = 123$ K.

Atomic parameters					
Atom	Site	symmetry	<i>x</i>	<i>y</i>	<i>z</i>
P1	4 <i>i</i>	<i>m</i>	0.1521(4)	0	0.7613(10)
P2	4 <i>i</i>	<i>m</i>	0.2861(6)	0	0.4331(5)
P3	8 <i>j</i>	1	0.3568(4)	0.1302 ^a	0.7580(6)
Displacement parameter, U_{ij} (Å ²)					
P ₄ (rigid body) ^b	U_{11}	U_{22}	U_{33}	U_{13}	
	0.054(2)	0.057(2)	0.036(1)	0.015(2)	

E.s.d.'s (1σ) are in parentheses

a: Deduced from the constraint on intramolecular P–P distances, $d(\text{P1–P2}) = d(\text{P3–P3})$

b: Calculated from the TLS matrix

validated by Rietveld refinement [15] of the fractional coordinates obtained at the end of the simulated annealing run. Although this run started from a general position, all runs ended with the P₄ moiety located in a single orientation with the molecular mirror plane congruent to the mirror plane of *Cm* resp. *C2/m* space group symmetry. *C2/m* could be confirmed as the appropriate space group by the structure determination and consecutive Rietveld refinement.

2.6 Rietveld refinement

Rietveld refinements were performed using the program GSAS [16]. The peak profile was described by a pseudo-Voigt function in combination with a special function that accounts for the asymmetry due to axial divergence [17,

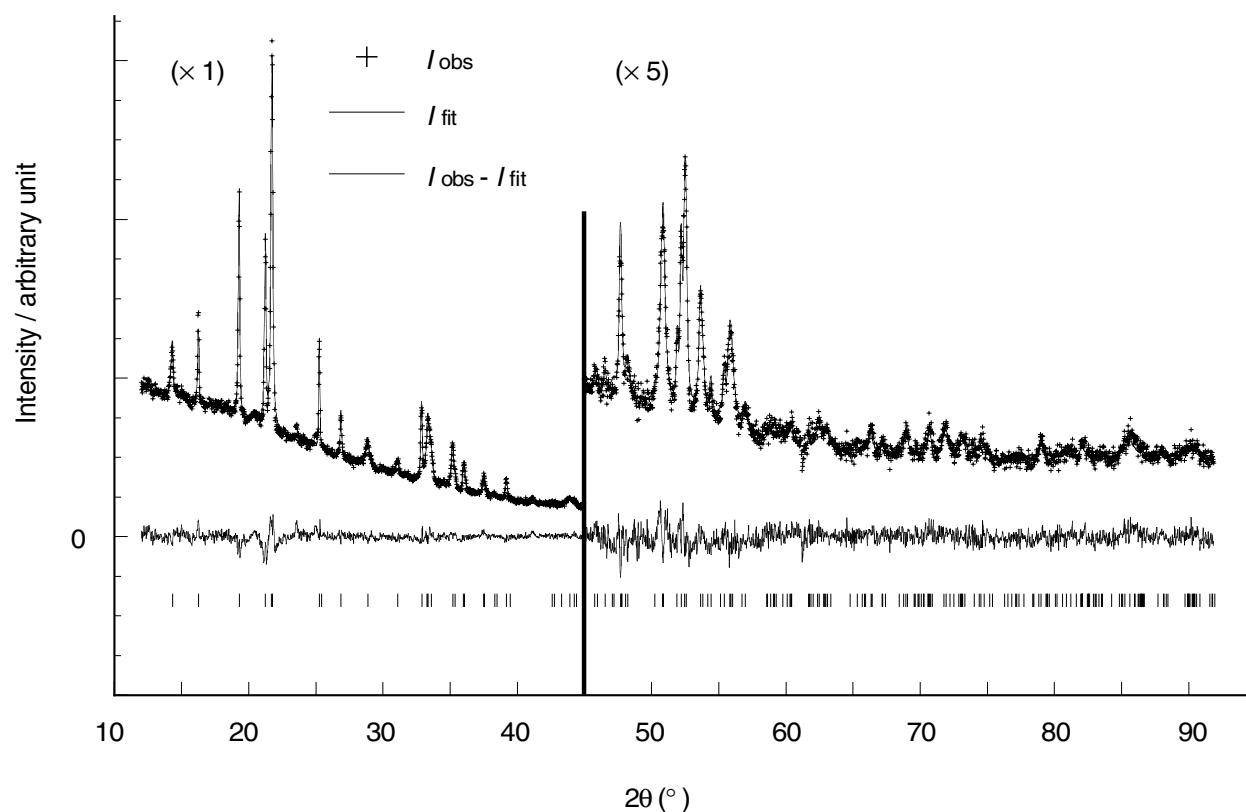


Fig. 3. Diffraction pattern of γ -P₄ and its fitting by Rietveld refinement. (Top) Observations (crosses) and calculated profile (solid line); (middle) difference between observations and calculated profile; (bottom) peak positions. The intensities in the 2θ region higher than 45° are magnified by a factor of 5 for clarity.

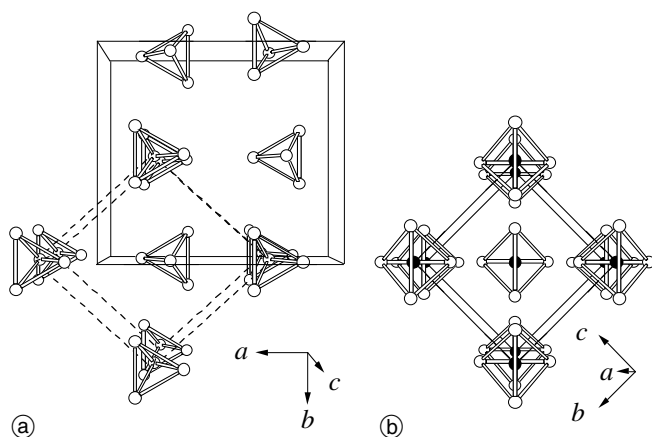


Fig. 4. (a) Crystal structure of γ -P₄ projected along [001]. P₄ molecules are shown as tetrahedra with P atoms at their apices. The monoclinic unit cell (solid lines) and the pseudo-bcc unit cell (dashed lines) are shown. (b) Unit cell of GeF₄ projected along [100].

18]. Background was slightly underdetermined manually and then adjusted using a cosine Fourier series with 8 coefficients. Anisotropic peak broadening mainly caused by lattice strain was observed with the broadest peaks along the *b*-direction. The phenomenological microstrain model of Stephens [19], as implemented in GSAS with 9 refinable parameters for monoclinic symmetry was used to model the anisotropy in full-width at half-maximum (FWHM) of the individual peak profiles. The isosurface of the anisotropic microstrain is given in Fig. 2. A rigid body for the P₄ tetrahedron was set up in a way allowing for a stretch/shrink of it along one axis. This axis was on the mirror plane and ran through midpoints of two edges (P1–P2 on the mirror plane and P3–P3' normal to the plane) of the tetrahedron. The TLS notation was used for the refinement of thermal vibrations [20]. All the atomic sites were assumed to be fully occupied. An unconstrained refinement of the three phosphorus atoms in the asymmetric unit resulted in small and meaningless distortions of the P₄ tetrahedron without improving the weighted profile agreement factor. In addition, least-squares cycles converged with negative values for some of the diagonal elements of anisotropic displacement tensors, U_{ii} . Therefore, the coordinates derived from the rigid body refinement were used. The conditions and results of the Rietveld refinement are given in Tables 1 and 2; the Rietveld plot is shown in Fig. 3 and the perspective view of the structure of γ -P₄ in Fig. 4.

3. Discussion

3.1 Structure of γ -P₄

The phosphorus atoms in γ -P₄ form almost perfect tetrahedra. According to a simple view of chemical bonding in the molecule lone pairs at the P atoms point away from the tetrahedron. Two phosphorus atoms within a tetrahedron are related by mirror symmetry. All other tetrahedra within the unit cell are created by space group symmetry. The unit cell is monoclinic with near to orthorhombic metrics, $\Delta\beta \approx 0.3^\circ$. The centers of gravity of the P₄ mole-

cules form distorted hexagon nets, the individual hexagons having chair conformation (Fig. 5a). The nets are congruently stacked in *c*-direction, and in consequence these molecules form a distorted body-centered cubic (bcc) packing (Fig. 4a). The central P₄ molecule in this cell is shifted quite significantly out of the center.

The identification of an approximate bcc structure of γ -P₄ allows a direct comparison with crystal structures that have an exact bcc arrangement of tetrahedral molecules as found for cubic SiF₄ [21], and GeF₄ [22]. The appropriate projection of the crystal structure of GeF₄ is compared with that of γ -P₄ in Figure 4. In the crystal structures of the tetrafluorides the tetrahedra are oriented in a way that the apices point towards the faces of adjacent tetrahedra which results in a coordination of each F atom by six F atoms from intermolecular contacts. The arrangement of the tetrahedra in γ -P₄ differs in so far, as the molecules are rotated in the mirror plane such that the apices of the tetrahedra point towards the large voids between neighbor-

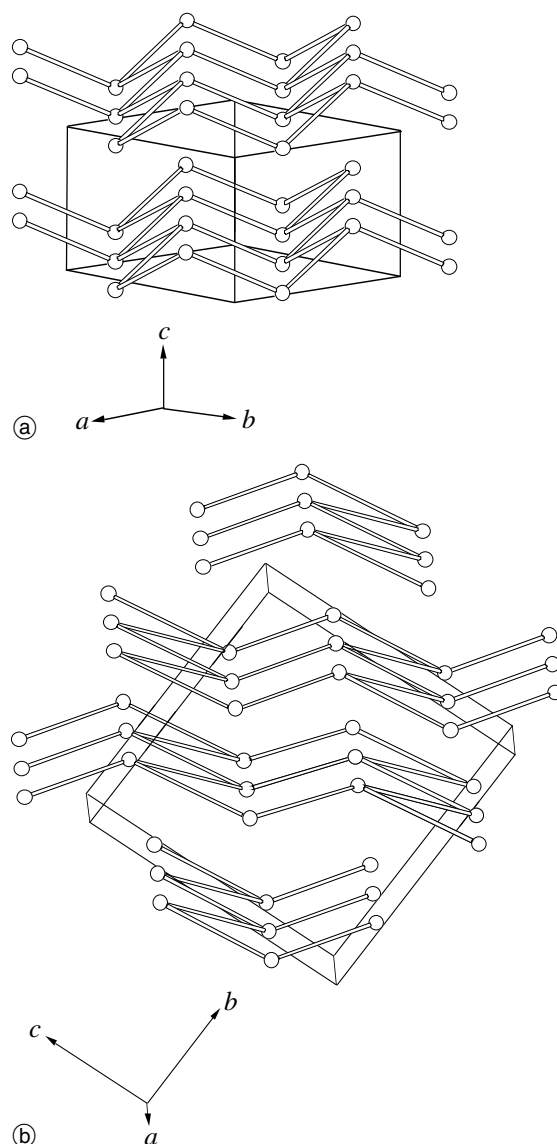


Fig. 5. Arrangements of P₄ molecules in γ -P₄ (a) and β -P₄ (b) showing only the centers of gravity of the P₄ tetrahedra. The unit cells are drawn. Hexagons with chair-conformation as the common structural element are clearly visible.

ing tetrahedra. In consequence, there are 12 P atoms from neighboring molecules coordinating to P1 (3.8 to 4.3 Å), 13 atoms to P2 (3.5 to 4.3 Å), and 12 atoms to P3 (3.5 to 4.4 Å) in addition to the three atoms within the molecule at distances of 2.17 Å. Clearly, the coordination numbers including the intramolecular neighbors, 15, 16 and 15, respectively of the P atoms in γ -P₄ is higher than that of the F atoms to alike ones in GeF₄ and to the coordination number 12 in the crystal structure of SnI₄ which has an fcc arrangement of the I atoms [23], reminding of tetrahedra packings in Frank-Kasper phases. The above mentioned shift of the central molecule in the crystal structure of γ -P₄ avoids a too close approach between P1 atoms (3.82 Å). The small tilt of two neighboring P₄-molecules in the *ac*-plane minimizes the interaction of the lone pairs of these atoms pointing approximately towards each other and determines the degree of monoclinic distortion.

The crystal packing and in particular the monoclinic distortion of γ -P₄ can be understood from maps showing areas of low and high electron localization as calculated by the electron localization function (ELF) using the LMTO method in the program STUTTGART TB-LMTO-ASA [24]. The ELF maps (Fig. 6) clearly show that the P₄ molecules are arranged in a way which optimizes van-der-Waals interaction as can be seen by the even distribution of low ELF density between the tetrahedra. This microscopic picture is completed by analyzing the isosurface of the anisotropic microstrain with its “softest directions”

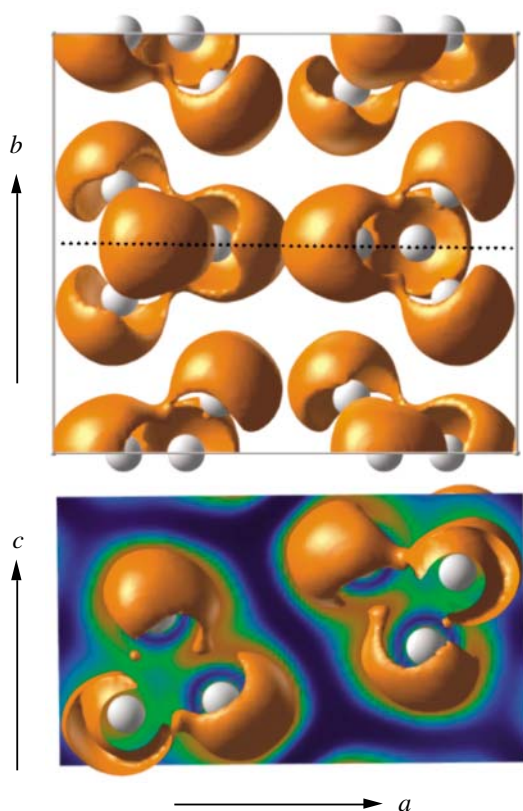


Fig. 6. Isosurfaces of the electron localization function (ELF) for γ -P₄ at $T = 123$ K in two projections. Brown shells show the surface of ELF = 0.8. ELF is almost zero in the inter-shell region that is shown in green to deep-blue (bottom) or left vacant (top). Gray balls show the positions of P atoms. The dashed line in the projection at the top indicates the position of the cut presented at the bottom.

located along $a \pm b$ (Fig. 2) which reflects the strong shear strain of neighboring P₄ molecules along the face diagonals.

3.2 Structural relationship between β - and γ -P₄

The arrangement of the P₄ molecules in γ -P₄ is similar to that in β -P₄ which in turn is similar to the atomic arrangement in γ -Pu [25]. In β -P₄, the P₄ molecules also form distorted hexagon nets stacked in [101] with respect to the triclinic unit cell (Fig. 5b). As in γ -P₄, the hexagons show up in chair conformation, too, however with much less deviation from planarity but stronger distortion of the hexagon within the net.

The relationship between the β - and γ -P₄ structures is clearly seen by seeking for directions which allow a description in terms of sets of planar quasi-3⁶ nets. Figure 7 shows another way of stacking such triangular nets formed by the centers of gravity of P₄ molecules. The γ -P₄ structure (Fig. 7a) is a periodic stacking of triangular nets A

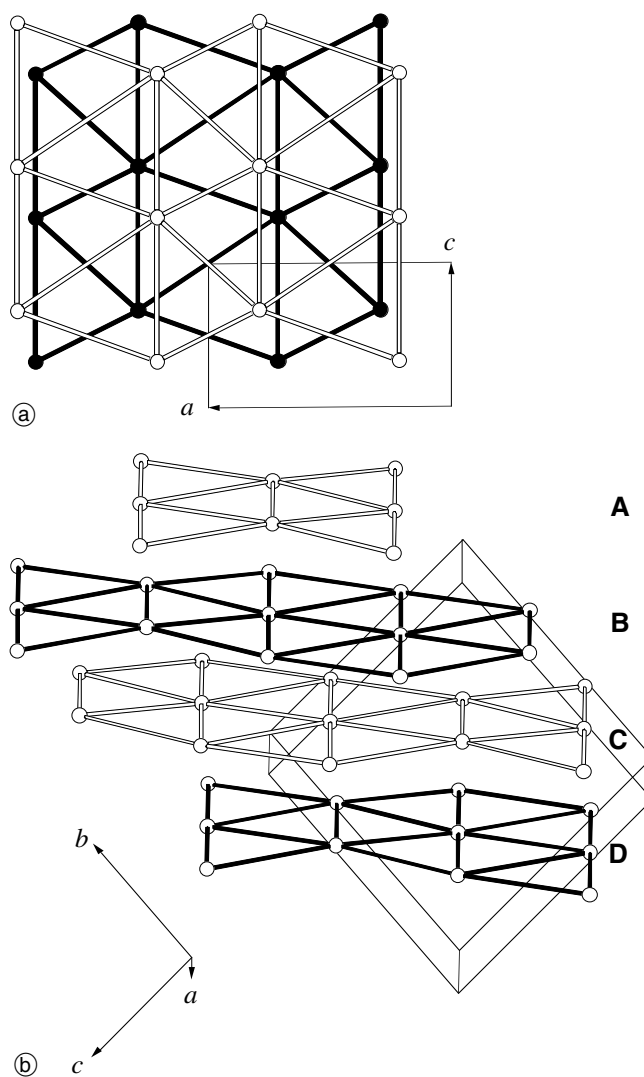


Fig. 7. Packing of P₄ molecules in γ -P₄ (a) and β -P₄ (b) as stacking of flat quasi-triangular nets formed by the centers of gravity of the P₄ tetrahedra. *a*: Filled and open rods show nets which lie at $y = 0$ (net A) and $y = 1/2$ (net B), respectively. *b*-axis is out of the plane of paper. *b*: Open rods show quasi-triangular nets A and C, and filled rods show nets B and D.

and B at $y = 0$ and $1/2$, respectively. Each P_4 molecule in net B is projected on net A near the midpoints of triangle edges along [001].

As it was discussed in Ref. [3], the β - P_4 structure (Fig. 7b) is also a periodic stacking of four nearly planar triangular nets in the sequence ABCD in the direction [0 $\bar{1}$ 1] of the triclinic cell. As shown in Figure 7b the couple A, B is identical to C, D except for a translation along [011]. Net A (C) is stacked upon B (D) in the same way as in the structure of γ - P_4 . Each P_4 molecule lies above the approximate midpoint of a triangle edge along [100] between two molecules in net B (D). Similarly, each P_4 molecule in net B can be projected on net C at the approximate midpoint of a triangle edge which, however, is now oriented along [1 $\bar{1}$ 1]. Hence, nets A and C are not related via a mirror symmetry as the next nearest nets in β - P_4 , but via an approximate rotation by 60° around an axis parallel [0 $\bar{1}$ 1] passing through the center of a molecule on net B. The relation between nets B and D with respect to C is characterized by a -60° rotation.

The γ to β transformation could be achieved easily by sliding AB (CD) stacks halfway along the quasi-triangle edge oriented parallel either [101] or [10 $\bar{1}$] in the γ - P_4 monoclinic cell corresponding to [211] in the β - P_4 triclinic cell, accompanied by relative reorientations of the molecules. However, as the phase transition from always randomly oriented micrograins in γ - P_4 proceeds to highly textured β - P_4 the mechanism of the transition can not be that simple.

Acknowledgments. Special thanks are due to Dr. Ullrich Wedig for the ELF calculations, Professor Hans Georg von Schnering and Dr. Jürgen Köhler for helpful discussions, and Roland Eger for experimental assistance. Support by the Fonds der Chemischen Industrie (FCI) is gratefully acknowledged.

References

- [1] Schnering, H. G. v.: Homoatomic bonding of main group elements. *Angew. Chem. Int. Ed. Engl.* **20** (1981) 33–53.
- [2] Bridgman, P. W.: Two new modifications of phosphorus. *J. Am. Chem. Soc.* **36** (1914) 1344–1363.
- [3] Simon, A.; Borrmann, H.; Horakh, J.: On the polymorphism of white phosphorus. *Chem. Ber./Recueil* **130** (1997) 1235–1240.
- [4] Spiess, H. W.; Grosescu, R.; Haeberlen, U.: Molecular motion studied by NMR powder spectra. 2. Experimental results for solid P_4 and solid $Fe(CO)_5$. *Chem. Phys.* **6** (1974) 226–234.
- [5] Simon, A.: Untersuchungen mit einer neuen Röntgenkamera: Phasenumwandlungen in festem Bromwasserstoff. *J. Appl. Crystallogr.* **4** (1971) 138–145.
- [6] Simon, A.: Das metallreichste Cäsiumoxid – Cs_7O . *Z. anorg. Allg. Chem.* **422** (1976) 208–218.
- [7] Okada, Y.; Tokumaru, Y.: Precise determination of lattice parameter and thermal expansion coefficient of silicon between 300 and 1500 K. *J. Appl. Phys.* **56** (1984) 314–320.
- [8] Toraya, H.: Array-type universal profile function for powder pattern fitting. *J. Appl. Crystallogr.* **23** (1990) 485–491.
- [9] Toraya, H.: Whole-powder-pattern fitting without reference to a structural model: Application to X-ray powder diffraction data. *J. Appl. Crystallogr.* **19** (1986) 440–447.
- [10] Shirley, R.: The CRYSFIRE System for Automatic Powder Indexing: User's Manual, The Lattice Press, 41 Guildford Park Avenue, Guildford, Surrey GU2 5NL, England.
- [11] David, W. I. F.; Shankland, K.; Shankland, N.: Routine determination of molecular crystal structures from powder diffraction data. *Chem. Commun.* (1998) 931–932.
- [12] Kirkpatrick, S.; Gelatt, C. D. Jr.; Vecchi, M. P.: Optimization by simulated annealing. *Science* **220** (1983) 671–680.
- [13] Pawley, G. S.: Unit-cell refinement from powder diffraction scans. *J. Appl. Crystallogr.* **14** (1981) 357–361.
- [14] Learch, A. R.: *Molecular modeling principles and applications*. Addison-Wesley Longman, Reading, MA, (1996) pp. 2–4.
- [15] Rietveld, H. M.: A profile refinement method for nuclear and magnetic structures. *J. Appl. Crystallogr.* **2** (1969) 65–71.
- [16] Larson, A. C.; von Dreele, R. B.: GSAS (1994) Version 2002. Los Alamos National Laboratory Report LAUR 86–748.
- [17] Thompson, P., Cox, D. E.; Hastings, J. B.: Rietveld refinement of Debye-Scherrer synchrotron X-ray data from Al_2O_3 . *J. Appl. Crystallogr.* **10** (1987) 79–83.
- [18] Finger, L. W.; Cox, D. E.; Jephcoat, A. P.: A correction for powder diffraction peak asymmetry due to axial divergence. *J. Appl. Crystallogr.* **27** (1994) 892–900.
- [19] Stephens, P. W.: Phenomenological model of anisotropic peak broadening in powder diffraction. *J. Appl. Crystallogr.* **32** (1999) 281–289.
- [20] Dinnebier, R. E.: Rigid bodies in powder diffraction. A practical guide. *Powder Diffraction* **14** (1999) 84–92.
- [21] Atoji, M., Lipscomb, W.: The structure of SiF_4 . *Acta Crystallogr.* **7** (1954) 597.
- [22] Köhler J., Simon, A., Hoppe, R.: Über die Kristallstruktur von GeF_4 . *J. Less-Common Met.* **137** (1988) 333–341.
- [23] Meller, F., Fankuchen, I.: The Crystal Structure of Tin Tetraiodide. *Acta Crystallogr.* **7** (1954) 343–344.
- [24] Jepsen, O.; Andersen, O.K.: The STUTTGART TB-LMTO-ASA program version 47 (2000) <http://www.mpi-stuttgart.mpg.de/andersen/>
- [25] Zachariasen, W. H.; Ellinger, F. H.: Crystal chemical studies of the $5f$ -series of elements. XXIV. The crystal structure and thermal expansion of γ -Plutonium. *Acta Crystallogr.* **8** (1955) 431–433.